Aerosol Science and Technology
Publication details, including instructions for authors and subscription information:
http://www.informaworld.com/smpp/title~content=t713656376

Modeling New Particle Formation During Air Pollution Episodes: Impacts on Aerosol and Cloud Condensation Nuclei

R. E. P. Sotiropoulou [ab]; E. Tagaris [ac]; C. Pilinis [a]; T. Anttila [de]; M. Kulmala [f]
[a] Department of Environment, University of the Aegean, University Hill, Lesvos, Greece
[b] Department of Earth and Atmospheric Sciences, Georgia Institute of Technology, Georgia, USA
[c] Department of Civil and Environmental Engineering, Georgia Institute of Technology, Georgia, USA
[d] Finnish Meteorological Institute, Air Quality Research, Helsinki, Finland
[e] ICG-II: Troposphäre, Forschungszentrum, Jülich, Germany
[f] Department of Physical Sciences, University of Helsinki, Helsinki, Finland

First Published on: 01 July 2006
To cite this Article: Sotiropoulou, R. E. P., Tagaris, E., Pilinis, C., Anttila, T. and Kulmala, M. (2006) 'Modeling New Particle Formation During Air Pollution Episodes: Impacts on Aerosol and Cloud Condensation Nuclei', Aerosol Science and Technology, 40:7, 557 - 572
To link to this article: DOI: 10.1080/02786820600714346
URL: http://dx.doi.org/10.1080/02786820600714346

Aerosol Science and Technology, 40:557–572, 2006

ISSN: 0278-6826 print / 1521-7388 online
DOI: 10.1080/02786820600714346

Modeling New Particle Formation During Air Pollution Episodes: Impacts on Aerosol and Cloud Condensation Nuclei

R. E. P. Sotiropoulou,[1,2] E. Tagaris,[1,3] C. Pilinis,[1] T. Anttila,[4,5] and M. Kulmala[6]

[1]*Department of Environment, University of the Aegean, University Hill, Lesvos, Greece*
[2]*Department of Earth and Atmospheric Sciences, Georgia Institute of Technology, Georgia, USA*
[3]*Department of Civil and Environmental Engineering, Georgia Institute of Technology, Georgia, USA*
[4]*Finnish Meteorological Institute, Air Quality Research, Helsinki, Finland*
[5]*ICG-II: Troposphäre, Forschungszentrum Jülich, Germany*
[6]*Department of Physical Sciences, University of Helsinki, Helsinki, Finland*

The impact of new particle formation on regional air quality and CCN formation is for the first time explored using the UAM-AERO air quality model. New particles are formed by ternary nucleation of sulfuric acid, ammonia and water; subsequent growth of clusters to large sizes is driven by condensation of sulfuric acid and organic vapors, as described by the recently developed nano-Köhler theory. Application of the model in Athens (GAA) and Marseilles (GMA) reveals higher sulfuric acid condensational sink and gaseous sulfuric acid (hence nucleation rate) for the latter. However, limited quantities of organic vapors in the GMA inhibit the growth of the formed clusters; therefore new particle formation is more efficient in the GAA. A sensitivity analysis demonstrates that (1) uncertainty in vaporization enthalpy does not affect organic carbon formed by nucleation, and (2) an accommodation coefficient of unity gives excellent agreement of condensation sink with in-situ observations. Nucleation affects the aerosol size distribution, and can be an important contributor to CCN; locally it can be more important than chemical ageing of pre-existing aerosols.

INTRODUCTION

Atmospheric aerosols and their role on air quality and climate have motivated a vast amount of research in the scientific community (Zhang et al. 2000; IPCC 2001). Predicting new particle formation is essential since nucleation affects climate and visibility by changing the aerosol size distribution (Charlson et al. 1987; Kulmala et al. 2000) and the cloud condensation nuclei (CCN) concentrations (O'Dowd et al. 2002), while ultrafine particles are likely to cause adverse health effects (e.g., Schwartz et al. 1996; Peters et al. 1997). Numerous theories have been developed to represent nucleation under typical tropospheric conditions; the most widely used is the homogeneous heteromolecular nucleation of water and sulfuric acid (e.g., Kulmala and Laaksonen 1990; Weber et al. 1999). To explain the high nucleation rates observed in the atmosphere (e.g., Stanier et al. 2004) a ternary water-sulfuric acid-ammonia formulation has been developed (O'Dowd et al. 1999; Kulmala et al. 2000). Ion-induced nucleation (Yu and Turco 2000; Kim et al. 2002) is very important for the upper troposphere and lower stratosphere, but its importance for lower tropospheric aerosol is likely to be secondary. Condensation, coagulation, and heterogeneous reactions (Yu and Turco 2000; Zhang and Wexler 2002; Jang et al. 2003; Laakso et al. 2003; Kerminen et al. 2001) are responsible for the subsequent growth of nucleated clusters.

New particle formation can affect the Earth's radiative budget by increasing the number of particles that serve as CCN (e.g., Lin and Chameides 1993; O'Dowd et al. 2002; Laaksonen et al. 2005). Increased CCN can increase the cloud droplet number concentration (CDNC), decrease the cloud effective radius which modifies the cloud optical properties (Twomey et al. 1974) and increase cloud lifetime (aerosol indirect effects). A number of studies investigate the impact of nucleation on CCN concentrations in coastal areas (e.g., O'Dowd et al. 2002; Pirjola et al. 2002). These studies suggest that in coastal regions a significant fraction of the new particles can grow into CCN, increasing CCN concentrations by more than 100% for critical supersaturation more than 0.35%. To date there is no relevant work for urban

Received 17 May 2005; accepted 23 March 2006.

The authors gratefully acknowledge Dr. Athanasios Nenes (Georgia Institute of Technology) for his time and effort in rewriting this manuscript, his help in the sensitivity analysis as well as for his suggestions to include the CCN study. We would also like to thank the reviewers whose comments led to significant improvements of the paper. This study is part of the project "Biogenic Aerosols and Air Quality in the Mediterranean Area" and is supported by EU through grant EVK2-CT-2001-00107 (BOND) of Directorate D16.

Address correspondence to C. Pilinis, Department of Environment, University of the Aegean, University Hill, 81100 Mytilene, Lesvos, Greece. E-mail: xpil@aegean.gr

environments, and needs to be addressed, since urban plumes have large scale impacts on aerosol microphysics.

Nucleation is an essential component of any air quality and global model that includes aerosol microphysics (e.g., Schell et al. 2001; Adams and Seinfeld 2002; Griffin et al. 2002; Kirkevåk and Iversen 2002). The most recent version of the Comprehensive Air Quality model with Extensions (CAMx; v4.10s) employs the Russell et al. (1994) nucleation parameterization in which the nucleation rate is calculated from the available sulfuric acid at each time step (ENVIRON 2004). New particle formation in the CIT (California Institute of Technology) three-dimensional urban/regional atmospheric model is based on the binary sulfuric acid-water homogeneous nucleation (Meng et al. 1998). Models-3/CMAQ, employs a parameterized form of binary sulfuric acid-water (EPA 1999) nucleation. In all these models, gas phase sulfuric acid concentration necessary for calculating the nucleation rate is determined by the oxidation of gas-phase sulfur dioxide; the nucleated mass is then assigned to the first section of the aerosol size distribution. No urban airshed models to date have included ternary nucleation, nor have they assessed the impact on CCN concentrations.

This study focuses on the impact of new particle formation on regional air quality and CCN concentrations. Simulations were carried out with the UAM-AERO model (Sonoma Technology 1996), with appropriate modifications to include parameterizations for nucleation and the subsequent growth of nuclei. The nucleation rate is calculated from a state-of-the-art ternary parameterization that depends on temperature and the concentrations of ammonia, sulfuric acid, and water vapor (Napari et al. 2002a, b). The advantage of incorporating a ternary nucleation module is that it performs better when estimating the high atmospheric particle formation rates compared to the predictions of the binary nucleation mechanism. The mass of freshly-nucleated particles growing to the smallest size explicitly treated by UAM-AERO was calculated on the basis of the parameterization developed by Kerminen et al. (2004), which takes into account the loss of nucleated clusters through coagulation scavenging by pre-existing particles as well as the cluster growth through condensation of sulfuric acid and water-soluble organic vapors. The enhanced UAM-AERO model is then applied for Athens, Greece, and Marseille, France, greater areas. These areas are characterized by large meteorological and land use diversity and are an ideal test for assessing the impact of nucleation on air quality. The CPU requirements of these two modules are minimal, increasing the average simulation time by 5–10%.

MODEL DESCRIPTION

The 3-D Photochemical Modeling Tool

The UAM-AERO model (Sonoma Technology 1996) is a gas/aerosol model that is based on the UAM-IV air quality model (SAI 1990a, 1990b, 1990c, 1990d, 1990e). The current version of UAM-AERO uses the SAPRC90 (Carter 1990) chemical mechanism, which is comprised of fifty chemical species (eleven fast reacting, thirty slow reacting, seven steady state, and two constant species, CH_4, H_2O), actinic flux and one hundred thirty chemical reactions. Primary emissions of organic compounds are assigned to nine lumped classes. The chemical mechanism simulates the production of secondary organic aerosol (SOA) from the oxidation of VOCs. The yield of biogenic compounds (terpenes) to condensable organics in the original UAM-AERO model was constant for all their reactions, namely, 762 μg m^{-3} condensable organic compounds per ppm of biogenic compound. However, in the framework of the Biogenic Aerosols and Air Quality in the Mediterranean Area (BOND) project (Bartzis et al. 2004; Sotiropoulou et al. 2004a, 2004b), UAM-AERO underwent major modifications to include a variable yield based on targeted smog chamber and field experiments. For the organics formed by the oxidation of biogenic compounds, the yield depends on both the temperature, T, and the pre-existing organic mass, M_o (Odum et al. 1996):

$$Y = M_o \sum_i \frac{\alpha_i K_i}{1 + K_i M_o} \qquad [1]$$

where α_i is the individual formation yield for oxidation product i, and K_i is the corresponding absorption equilibrium constant. The$K$-values are expressed as

$$K_i(T) = K_i \left(\frac{T}{T_{ref}}\right) \exp\left[\frac{H}{R}\left(\frac{1}{T} - \frac{1}{T_{ref}}\right)\right] \qquad [2]$$

where $T_{ref} = 35^\circ$C, R is the ideal gas constant (0.0019872 kcal mol^{-1} K) and H is the enthalpy of vaporization of products [10–25 kcal mol^{-1} in most experiments, (Sheehan and Bowman 2001)].

Since ambient air consists of several monoterpenes that exhibit a wide range of SOA yields, a lumping of monoterpenes based on global emissions of the most important VOCs was necessary. Moreover, the reaction rates for the reactions of terpenes with ozone, nitrate radicals and hydroxyl radicals have been recalculated based on the abundance of biogenic compounds in the regions of interest (Breinbjer et al. 2003; Larsen et al. 2003). The yields and the enthalpies embodied into the model along with the modified reaction rates are summarized in Table 1.

Regarding aerosols, their size distribution treatment in the UAM-AERO model is based on a fractional representation with user-applied size bins. For the simulation of the aerosols-size distribution a number of 8 size sections from 0.04 to 10 μm for aerosols was used. All primary and secondary components of atmospheric particulate matter (sulfate, nitrate, ammonium, chloride, sodium, elemental carbon (EC), organic carbon (OC), water, and other crystal materials (OTR)) are treated. The default geometric mass mean diameters proposed by UAM-AERO (Sonoma Technology 1996) were used for the aerosol species. In particular, the mean diameters used are 1.3 μm for $SO_4^=$,

TABLE 1
Formation yields and partitioning coefficients for the lumped category of biogenic compounds used in the UAM-AERO model

Reaction	Reaction rates	Yield	Enthalpy H
Terpenes + OH	A = 36428 (ppm min)$^{-1}$	$\alpha_1 = 0.35$	17
		$\alpha_2 = 0$	
	B = −0.807	$K_1 = 0.08$	
		$K_2 = 0$	
Terpenes + O_3	A = 2.267 (ppm min)$^{-1}$	$\alpha_1 = 0.235$	17
		$\alpha_2 = 0.29$	
	B = 1.630	$K_1 = 0.05$	
		$K_2 = 0.0063$	
Terpenes + NO_3	A = 2413 (ppm min)$^{-1}$	$\alpha_1 = 1.0$	17
		$\alpha_2 = 0$	
	B = 0.849	$K_1 = 0.0115$	
		$K_2 = 0$	

1.2 μm for NO_3^-, 1.1 μm for NH_4^+, 2.4 μm for Na^+, 1.7 μm for Cl^-, 1.8 μm for OC, 1.6 μm for EC, 2.1 μm for OTR, 1.5 μm for H_2O, and 1.6 μm for H^+ under non-fog conditions. The physical processes considered in the simulations are: advection, turbulent diffusion, condensation and evaporation, coagulation, emissions, and deposition, while the nucleation process in the original version of the model was neglected. Particle growth and shrinkage were determined by the equilibrium concentrations calculated by ISORROPIA (Nenes et al. 1998, 1999), which considers 26 species (4 gas phase, 13 liquid phase and 9 solid phase) and has been chosen for its computational efficiency and comprehensive treatment of aerosol thermodynamics. A detailed description of UAM-AERO can be found in Sotiropoulou et al. (2004a).

The Nucleation Parameterization

Thermodynamically stable clusters are assumed to form through ternary nucleation of sulfuric acid, ammonia, and water, using the parameterization of Napari et al. (2002a, b). The nucleation rate, $J(d_p^*)$, depends on the temperature, T, the relative humidity, RH, the concentration of sulfuric acid, c, and the ammonia mixing ratio, ξ.

$$\begin{aligned}\ln J(d_p^*) = {} & -84.7551 + \frac{f_1(T)}{\ln c} + f_2(T)\ln c + f_3(T)\ln^2 c \\ & + f_4(T)\ln\xi + f_5(T)\ln^2\xi + f_6(T)RH \\ & + f_7(T)\ln RH + f_8(T)\frac{\ln\xi}{\ln c} + f_9(T)\ln\xi\ln c \\ & + f_{10}(T)RH\ln c + f_{11}(T)\frac{RH}{\ln c} + f_{12}(T)RH\ln\xi \\ & + f_{13}(T)\frac{\ln RH}{\ln c} + f_{14}(T)\ln RH\ln\xi \\ & + f_{15}(T)\frac{\ln^2\xi}{\ln c} + f_{16}(T)\ln^2\xi\ln c \\ & + f_{17}(T)\ln\xi\ln^2 c + f_{18}(T)RH\ln^2\xi \\ & + f_{19}(T)\frac{RH\ln\xi}{\ln c} + f_{20}(T)\ln^2\xi\ln^2 c \end{aligned} \quad [3]$$

where each of the functions $f_i(T)$ is a third-order polynomial:

$$f_i(T) = a_{i0} + a_{i1}T + a_{i2}T^2 + a_{i3}T^3 \quad [4]$$

The coefficients α_{ij} are listed in Table 2.

In the above equations T is in K, c in cm^{-3}, ξ in ppt, RH takes values between 0 and 1 and $J(d_p^*)$ in cm^{-3} s^{-1}. The parameterization considers a wide range of gas abundances observed in the troposphere and relative humidities between 5 and 95%. For the above fitting, the applicable temperature range is somewhat limited, from 240–300 K (Napari et al. 2002b). The sulfuric acid concentration should range between 10^4 and 10^9 molecules cm^{-3}, while the ammonia mixing ratio should be between 0.1 and 100 ppt. The parameterization is valid for nucleation rates between 10^{-5} to 10^6 cm^{-3} s^{-1}. The upper limit of nucleation rate is particularly stringent due to the polynomial fit. More details about the limits of validity of the parameterization can be found at Napari et al. (2002b).

The number of molecules, n_i^*, of each species (i.e., H_2SO_4 or NH_3) found in the critical nucleus is given by the nucleation rate and temperature, (Napari et al. 2002):

$$\begin{aligned} n^*_{H_2SO_4} = {} & 38.1645 + 0.774106\ln J(d_p^*) \\ & + 0.00298879\ln^2 J(d_p^*) - 0.357605T \\ & - 0.00366358T\ln J(d_p^*) + 0.0008553T^2 \end{aligned} \quad [5]$$

$$\begin{aligned} n^*_{NH_3} = {} & 26.8982 + 0.682905\ln J(d_p^*) \\ & + 0.00357521\ln^2 J(d_p^*) - 0.265748T \\ & - 0.00341895T\ln J(d_p^*) + 0.000673454T^2 \end{aligned} \quad [6]$$

$$\begin{aligned} n^*_{tot} = {} & 79.3484 + 1.7384\ln J(d_p^*) + 0.00711403\ln^2 J(d_p^*) \\ & - 0.744993T - 0.00820608T\ln J(d_p^*) \\ & + 0.0017855T^2 \end{aligned} \quad [7]$$

$$\begin{aligned} r^* = {} & 0.141027 - 0.00122625\ln J(d_p^*) - 7.82211 \\ & * 10^{-6}\ln^2 J(d_p^*) - 0.00156727T \\ & - 0.00003076T\ln J(d_p^*) + 0.0000108375T^2 \end{aligned} \quad [8]$$

where r^* is the radius of the critical cluster (nm), n^*_{tot} are the total number of nucleated particles, T is in K, and $J(d_p^*)$ in cm^{-3} s^{-1}.

Parameterization of Nuclei Growth

Freshly nucleated clusters range between 1 and 3 nm in radius (Equation [8]), thus are too small for the aerosol sizes considered

TABLE 2
Coefficients of Polynomials *fi(T)* used in UAM-AERO for the estimation of the nucleation rate

i	α_{i0}	α_{i1}	α_{i2}	α_{i3}
1	−0.355297	−33.8449	0.34536	−0.000824007
2	3.13735	−0.772861	0.00561204	-9.74576×10^{-6}
3	19.0359	−0.170957	0.000479808	-4.14699×10^{-7}
4	1.07605	1.48932	−0.00796052	7.61229×10^{-6}
5	6.0916	−1.25378	0.00939836	−0.0000174927
6	0.31176	1.64009	−0.00343852	−0.0000109753
7	−0.0200738	−0.752115	0.00525813	-8.98038×10^{-6}
8	0.165536	3.26623	−0.0489703	0.000146967
9	6.52645	−0.258002	0.00143456	-2.02036×10^{-6}
10	3.68024	−0.204098	0.00106259	-1.2656×10^{-6}
11	−0.066514	−7.82382	0.0122938	0.0000618554
12	0.65874	0.190542	−0.00165718	3.41744×10^{-6}
13	0.0599321	5.96475	−0.0362432	0.0000493337
14	−0.732731	−0.0184179	0.000147186	-2.37711×10^{-7}
15	0.728429	3.64736	−0.027422	0.0000493478
16	41.3016	−0.35752	0.000904383	-5.73788×10^{-7}
17	−0.160336	0.00889881	−0.0000539514	8.39522×10^{-8}
18	8.57868	−0.112358	0.000472626	-6.48365×10^{-7}
19	0.0530167	−1.98815	0.0157827	−0.0000293564
20	−2.32736	0.0234646	−0.000076519	8.0459×10^{-8}

by UAM-AERO. Introducing an extra size bin, or, extending the range of the first (smallest size) bin of the model to critical cluster sizes could potentially allow the direct implementation of nucleation; this is a numerically challenging problem, as it would require a very small integration step size (growth rates due to coagulation and condensation are very large for small particles) for a numerically stable solution. This computationally expensive approach is circumvented by parameterizing the growth of freshly nucleated particles and predicting the fraction of nuclei that will grow to the aerosol size range of UAM-AERO (within the integration timestep).

Nano–Köhler theory (Kerminen et al. 2004) is the basis of the growth parameterization; freshly-nucleated clusters are allowed to grow up to their critical activation diameter, d_{crit}, by reversible sulfuric acid condensation (together with associated water and ammonia). Subsequent growth is then driven by irreversible condensation of both sulfuric acid and low-volatility organics. The parameterization requires knowledge of the nucleation rate, the condensational sink (i.e., the rate of condensation of low-volatility molecules onto pre-existing aerosols, calculated for the particle size range resolved in UAM-AERO) and the concentrations of condensing vapors. The "grown" nuclei are introduced as a source term in the smallest UAM AERO aerosol bin; this "apparent" nucleation rate, $J(d_p)$, is always smaller than the real nucleation rate, $J(d_p^*)$, due to coagulation of the growing clusters onto larger pre-existing particles (Kerminen et al. 2004) and non activation of all nano-particles. $J(d_p)$ can be related to $J(d_p^*)$ by assuming non-constant growth rate for nuclei and power law dependence of coagulation (Kerminen et al. 2004):

$$J(d_p, t') = J(d_p^*, t) \exp\left[\frac{\eta_{org}}{d_p} + \frac{\eta_{sul} - \eta_{org}}{d_{crit}} - \frac{\eta_{sul}}{d_p^*}\right] \quad [9]$$

where the factors η_{org} and η_{sul} in nm are given by:

$$\eta_{sul} = \frac{\gamma CS}{4\pi D_i GR_{sul}} \quad [10]$$

$$\eta_{org} = \frac{\gamma CS}{4\pi D_i (GR_{sul} + GR_{org})} \quad [11]$$

where γ is a proportionality factor in nm^2 m^2 h^{-1}, CS is the condensational sink in s^{-1}, D_i is the vapor diffusion coefficient in m^2 s^{-1}, and GR_{sul} and GR_{org} are the nucleus growth rates due to irreversible condensation of sulfuric acid and organic compounds in nm h^{-1}, respectively. CS can be calculated from the pre-existing particle size distribution:

$$CS = 2\pi D_i \sum_j \frac{d_{p,j} N_j \alpha (1 + Kn_j)}{\alpha + 0.377\alpha Kn_j + 1.33 Kn_j (1 + Kn_j)} \quad [12]$$

where $d_{p,j}$ is the mean diameter of the pre-existing particles in size section j, N_j is their number concentration, α the mass accommodation coefficient of the condensing vapor equal to

one, and $Kn_j = 2\lambda/d_{p,j}$ is the Knudsen number in which λ is the molecular mean free path. The growth rate of a cluster, GR (nm h^{-1}), is given by (Kerminen and Kulmala 2002):

$$GR = \frac{3.0 \times 10^{-9}}{\rho_{nuc}} \sum_i \bar{c}_i M_i C_i \quad [13]$$

where C_i (cm^{-3}) is the vapor concentration in the gas phase, ρ_{nuc} (kg m^{-3}) is the density of the cluster, $\overline{c_i}$ (m s^{-1}) is the molecular speed of the condensing vapor and M_i (g mol^{-1}) is its molecular weight.

The parameter γ (nm^2 m^2 h^{-1}) is calculated by Kerminen and Kulmala (2002):

$$\gamma = \gamma_0 \left[\frac{d_{nuc}}{1\text{ nm}}\right]^{0.2} \left[\frac{d_p}{3\text{ nm}}\right]^{0.075} \left[\frac{d_{mean}}{150\text{ nm}}\right]^{0.048} \times \left[\frac{\rho_p}{1\text{g cm}^{-3}}\right]^{-0.33} \left[\frac{T}{293\text{ K}}\right] \quad [14]$$

where γ_0 is equal to 0.23 nm^2 m^2 h^{-1}, d_{mean} is the number mean diameter (nm) of the pre-existing particle population (i.e., those particles with diameter larger than d_p), ρ_p is the density of the growing nuclei (g cm^{-3}). A semi-empirical formula for d_{crit} (m), was derived based on the work of Kerminen et al. (2004a).

$$d_{crit} = \frac{6.4898275 - 0.01555585T + 0.038826705\log(S_{org,crit})}{1 - 0.0019969989T + 0.17369093\log(S_{org,crit})} \quad [15]$$

where $S_{org,crit}$ is the organic vapor critical saturation ratio.

Since the concentrations of gas-phase organics and sulfuric acid change between time steps, the apparent nucleation rate and the diameter of the clusters are calculated over each time interval $[t, t']$ by the following equations:

$$\begin{aligned} d_{i+1} &= d_i + GR_{sul,i}\Delta t, \quad \text{if} \quad d_{i+1} < d_{crit} \\ d_{i+1} &= d_{crit} + GR_{org,i}\left(\Delta t + \frac{d_i - d_{crit}}{GR_{sul,i}}\right), \\ &\quad \text{if} \quad d_i < d_{crit} < d_{i+1} \\ d_{i+1} &= d_i + \left(GR_{sul,i} + GR_{org,i}\right)\Delta t, \quad \text{if} \quad d_i > d_{crit} \end{aligned} \quad [16]$$

$$J(d_{i+1}, t + \Delta t) = J(d_i, t)\exp\left[\frac{\eta_{sul,i}}{d_{i+1}} - \frac{\eta_{sul,i}}{d_i}\right] \quad \text{if} \quad (d_{i+1} < d_{crit})$$

$$J(d_{i+1}, t + \Delta t) = J(d_i, t)\exp\left[\frac{\eta_{org,i}}{d_{i+1}} + \frac{\eta_{sul,i} - \eta_{org,i}}{d_{crit}} - \frac{\eta_{sul,i}}{d_i}\right] \quad \text{if} \quad (d_i < d_{crit} < d_{i+1})$$

$$J(d_{i+1}, t + \Delta t) = J(d_i, t)\exp\left[\frac{\eta_{org,i}}{d_{i+1}} - \frac{\eta_{org,i}}{d_i}\right] \quad \text{if} \quad (d_{crit} < d_{i+1} < d_p)$$

$$J(d_p, t') = J(d_i, t)\exp\left[\frac{\eta_{org,i}}{d_p} - \frac{\eta_{org,i}}{d_i}\right] \quad \text{if} \quad (d_{i+1} > d_p) \quad [17]$$

In Equations (16) and (17), d_1 and $J(d_1)$ correspond to d_p^* and $J(d_p^*)$, respectively. A detailed description of the parameterization can be found in Kerminen et al. (2004).

Interface Between the Two Parameterizations and the UAM-AERO Model

The parameterizations of nucleation and subsequent growth of nuclei were embodied into the UAM-AERO model. In each time step the model first calculates the gas-phase concentrations of all the compounds resulting from transport and chemical reactions. Then, the condensational sink of sulfuric acid is calculated and consequently the quantity of sulfuric acid available for new particle formation. The nucleation module, using the predicted concentrations of ammonia, sulfuric acid available for nucleation, the temperature, and the relative humidity, examines whether the limits of the ternary nucleation parameterization are satisfied. If they are satisfied, the nucleation rates as well as the critical cluster size are calculated. If ammonia or sulfuric acid concentrations exceed the upper limits of the parameterization, the model uses values obtained with these upper limits. In contrast, when their concentrations are lower than the corresponding limits, nucleation doesn't take place. Regarding temperature and relative humidity, nucleation takes place only when these parameters are within the limits of the parameterization. In most cases studied, the limiting parameter is the sulfuric acid concentration followed by the upper limit of the temperature that is sometimes exceeded, particularly during noon in summer months.

After the inorganic nuclei formation, gaseous sulfuric acid, a small amount of water, and ammonia start to condense onto them in order to maintain a thermodynamic equilibrium between the gas phase and the growing nuclei. Initially the nuclei growth rate increases slightly with their size. When they grow further and become "activated," that is, exceed the critical diameter (with respect to organic vapors) both water soluble organic vapors and sulfuric acid are responsible for their growth. At this point, a significant increase in the growth rate is noted. This process is repeated for all cells in the domain at each time step. According to the parameterization, within the size range $[d_p^*, d_p]$ there are always (t′-t)/Δt populations of different-size nuclei. Equations (16) and (17) are applied separately to each of these populations. Depletion of gas-phase sulfuric acid and organic vapors inhibits new particle formation, since freshly nucleated clusters coagulate rapidly with pre-existing particles.

The nucleation and growth modules estimate the nuclei number concentrations. Using the growth rates from sulfuric acid and organic vapor condensation and the duration of each time step, the change of nucleus diameter caused by each compound at each time step can be calculated. Assuming a spherical shape for the nucleus, the increase in volume and subsequently its mass

for each population within the size range $[d_p^*, d_p]$ can be calculated. When a population or populations cross the lower diameter used by UAM-AERO, the total mass of sulfates and organics is calculated by multiplying the apparent nucleation rate of each population with the sum of masses from each time step. This new particle mass is introduced into the smallest size bin of the UAM-AERO aerosol module (in this work, 40 nm diameter). Thereinafter, the new and pre-existing aerosol masses are managed together by the model, and the simulation of aerosol species is performed.

Calculation of CCN Concentrations

The ability of atmospheric aerosol to act as cloud condensation nuclei (CCN) depends strongly on their composition and dry size (e.g., Seinfeld and Pandis 1998; Henning et al. 1999). Most particles with diameters larger than 30–50 nm can act as CCN under typical cloud formation conditions (e.g., Hegg 1990; Hudson and Da 1996; Shaw et al. 1998; Seinfeld and Pandis 1998; Lowenthal et al. 2002). Nucleation increases the number concentration of small particles and can potentially impact CCN concentrations (e.g., O'Dowd 2002); this is explored in our simulations.

Linking aerosol size and composition to CCN activity is done using Köhler theory (Köhler 1936); this theory derives the minimum ambient water vapor supersaturation required for an aerosol to act as a CCN and become a droplet. This "critical" superaturation, S_c, for a multicomponent CCN of dry diameter, d_{dry} (m) is given by (Seinfeld and Pandis 1998):

$$S_c = \left(\frac{4A^3}{27B}\right)^{\frac{1}{2}} \quad [18]$$

where $A = \frac{4M_w\sigma_w}{RT\rho_w}$ and $B = \frac{d_{dry}^3 M_w}{\rho_w}\sum_i \frac{\rho_{s,i}\nu_{s,i}\varepsilon_i}{M_{s,i}}$. M_w and $M_{s,i}$ are the molecular weights of water and solute in kg mol^{-1}, respectively, σ_w (J m^{-2}) is the surface tension of the solution, ε_i is the dissolved volume fraction, ρ_w and $\rho_{s,i}$ (kg m^{-3}) are the densities of water and aqueous solution, respectively, $\nu_{s,i}$ is the number of ions into which a solute molecule dissociates (Van't Hoff factor), R (J mol^{-1} K^{-1}) is the ideal gas constant, i represents all the water-soluble components of the aerosol. The volume fraction is given by:

$$\varepsilon_i = \frac{m_i/\rho_i}{\sum_j \frac{m_j}{\rho_j}} \quad [19]$$

where m_i is the mass fraction of component i, and j represents all the components in the aerosol (soluble and insoluble). ISORROPIA (Nenes et al. 1998, 1999) is used to attribute the inorganic ions into the mixture of salts used for the B term. After calculating the critical supersaturation of each section we compute the CCN that activate between 0.1 and 1.6% supersaturation.

In applying Equation (18), we assume that EC, OC, and crustals are insoluble. This assumption, although oversimplified, has been shown to give reasonable CCN closure (to within 25%) for polluted North American aerosol sampled during the International Consortium for Atmospheric Research on Transport and Transformation (ICARTT) experiment (July–August 2004) (Medina et al., in review; Sotiropoulou et al. 2006). The same assumption also yields good cloud droplet closure for clouds sampled during the Coastal Stratocumulus Imposed Perturbation Experiment (CSTRIPE, Monterey, California, July 2003) field experiments (Meskhidge et al. 2005). We assume that our CCN calculations would be subject to comparable uncertainty.

Application of the New Version of the UAM-AERO Model

Within the framework of the BOND project two Mediterranean areas were selected for study, Athens, Greece, and Marseilles, France. These areas were chosen because of the elevated biogenic emission levels and the sufficient degree of meteorological and land use diversity.

The modeling domain for the GAA include the Athens urban area, containing the bulk of the anthropogenic emissions, as well as an extended surrounding rural area with biogenic emissions. It extends from 93 km west to 91 km east and from 91 km south to 93 km north of the city of Athens, covering a total area of 33,856 km^2. The domain on which UAM-AERO was applied was a 92 × 92 grid system with horizontal grid increments of 2 km in both directions. In the vertical, 10 layers of variable thickness were used, up to 5,000 m above ground level, 6 under and 4 above the diffusion break, for both episodes. The domain was chosen in such a way that the boundary concentrations could be assumed to be background ones compared to the concentrations in the basin.

The GMA domain was selected by taking into account the geographic extension of the available topographical, land cover, anthropogenic, and biogenic emission data. It extends from 71 km west to 57 km east and from 57 km south to 79 km north of the city of Marseille and it covers an area of 17408 km^2. The domain on which UAM-AERO was applied was a 64 × 68 grid system, with horizontal grid increments of 2 km in both directions. In the vertical, 10 layers of variable thickness were used, up to 5,500 m above ground level, 6 under and 4 above the diffusion break, for all days. A detailed description of the domains of interest can be found in Sotiropoulou et al. (2004a).

During the BOND project, two field campaigns took place, one in Marseilles (between 1 and 19 July 2002) followed by a second in Athens (between 10 and 26 June 2003). During each campaign, the growth properties of nucleation mode particles were observed by the University of Helsinki (Kulmala et al. 2005). The measurement site in Athens was located in Thrakomakedones (38°8′37″ N, 23°45′29″ E, 550 m above sea level), approximately 20 km north from the Athens city centre in the foothills of mountain Parnitha. The monitoring station is surrounded by suburban areas in the south and evergreen forests in the north. For the GMA, the measurements were conducted at Plan d' Aups (43°19′ N, 5°42′ E, 700 m above

sea level), approximately 40 km northeast from Marseille city center.

For each domain, two multi-day episodes from the field campaigns were simulated. For each episode we simulate aerosol formation with and without nucleation. The meteorological fields are generated by the 3-D non-hydrostatic, fully compressible ADREA-I mesoscale prognostic model (Bartzis et al. 1991). For both domains, data from the literature were used as initial conditions for 24 gas species and eight aerosol constituents. However, in order to avoid any domination by the initial conditions onto the predictions, we used a spin up time of two days while a total simulation of four days was performed. The air quality was simulated in the Greater Marseilles Area (GMA) during the episode of 6–9 July 2002, and in the Greater Athens Area (GAA) during the 22–25 June 2003 episode. Gridded hourly anthropogenic emissions have been estimated based on traffic information and the industrial activities in the domain. Biogenic emissions of NO, NH_3, alkanes, olefins, ethene, isoprene, and terpenes at ground level were provided by the University of Louis Pasteur, France. Particularly for the GAA, in order to estimate ammonia emissions over the entire area, primary data concerning the animals, the types of cultivations, and the areas covered by them were obtained from the National Statistical Service of Greece as these are the three main categories that are responsible for the ammonia emissions in the GAA (Sotiropoulou et al. 2003).

RESULTS AND DISCUSSION

Aerosol Microphysics

To calculate new particle formation, we need the sulfuric acid condensational sink and the acid available for nucleation. Figure 1 presents the spatial distribution of the condensational sink for the GAA (Figure 1a) at 15:00(LST) on June 24, 2003, and for the GMA (Figure 1b) at 15:00 (LST) on July 8, 2002. These two figures express the combination of gas-phase sulfuric acid and area available for condensation. In the GAA (Figure 1a), during the morning hours the wind blows from N-NW. This results in higher condensational sink to be calculated to the NW and in a narrow part of the domain over the urban area of Athens due to SO_2 emissions from local sources. In GMA, higher condensational sink is calculated mainly SW due to the transport of SO_2 from the industrial area located in the center of the domain, as well as from the urban areas of Marseilles and Toulon located to the SE shores. Figure 1 also presents the spatial distribution of acid available for nucleation in the GAA (Figures 1c) and GMA (Figure 1d). The regions of low gas-phase acid availability are a result of high condensational sink and low acid production. This is reflected in the predicted nucleation rates for GAA (Figure 1e) and GMA (Figure 1f), respectively. The spatial distribution of the nucleation rate in both regions is similar to the distribution of the available sulfuric acid for nucleation, as it is the most important and usually limiting parameter in the nucleation process. Moreover, it reflects the concentration of newly formed clusters which is a strong function of the acid concentration, as long as ammonia, temperature, and humidity are within the range this parameterization is valid. Therefore the maxima are noted in areas with elevated concentrations of sulfuric acid under the condition that the rest of the parameters do not limit the whole process. The role of ammonia in the formation of new particles is very important for both domains as it enhances the nucleation rate (increase up to three orders of magnitude compared to the predictions of the model employing a binary nucleation module). However, nuclei are predicted to have a fairly acidic nature since the concentration of NH_3 in a nucleus is less than the corresponding concentration of H_2SO_4. This result is also confirmed by experimental data (Zhang et al. 2004). Thus the concentrations of NH_3 and NH_4^+ are not affected by the nucleation module. Higher values of the condensational sink of sulfuric acid are observed in the GMA than in the GAA due to the higher concentrations of pre-existing particles. Despite this, the higher SO_2 emissions result in higher sulfuric acid concentrations in the GMA, and, consequently, the nucleation rates are also higher therein.

The condensation parameterization was evaluated using the condensational sink and growth rate measurements obtained during the field campaigns (Kulmala et al. 2005). In general, particle growth rates range between 1 and 20 nm h^{-1} in mid-latitudes depending on the temperature and the availability of condensable vapors (Kulmala et al. 2004a). For the GAA, 7 events of nucleation and growth were observed. In these events new cluster growth rate ranges between 2.3 and 11.8 nm hr^{-1}, while the condensational sink varied between 5.8×10^{-3} and 1.3×10^{-2} s^{-1}. For the GMA, during the campaign 10 events were observed; the growth rate of new clusters was measured between 1.1 and 8.1 nm hr^{-1},while the condensational sink was measured between 3.2×10^{-3} and 1.5×10^{-2} s^{-1}. The calculated condensational sinks are shown in Figure 2 for the GAA (Figure 2a) and the GMA (Figure 2b); the predicted hourly growth rates are shown for the GAA and the GMA in Figures 2c and 2d, respectively. From the figures it can be seen that the condensational sinks calculated by the model as well as the calculated growth rates of nuclei are within the corresponding higher and lower values that have been measured. Although based upon a limited set of conditions, this result is important for evaluating the performance of the parameterizations and their coupling with the UAM-AERO model. Moreover, one should be cautious when comparing predicted and measured values, since the observed ones are at a fixed point, whereas the model predictions refer to the average value of the grid.

Despite the existence of clusters almost everywhere in the domains of interest, only a small fraction of them will manage to grow large enough to contribute to the PM. Experimental studies have shown the strong interplay between the nuclei growth and their loss by coagulation (Kulmala et al. 2005). In polluted

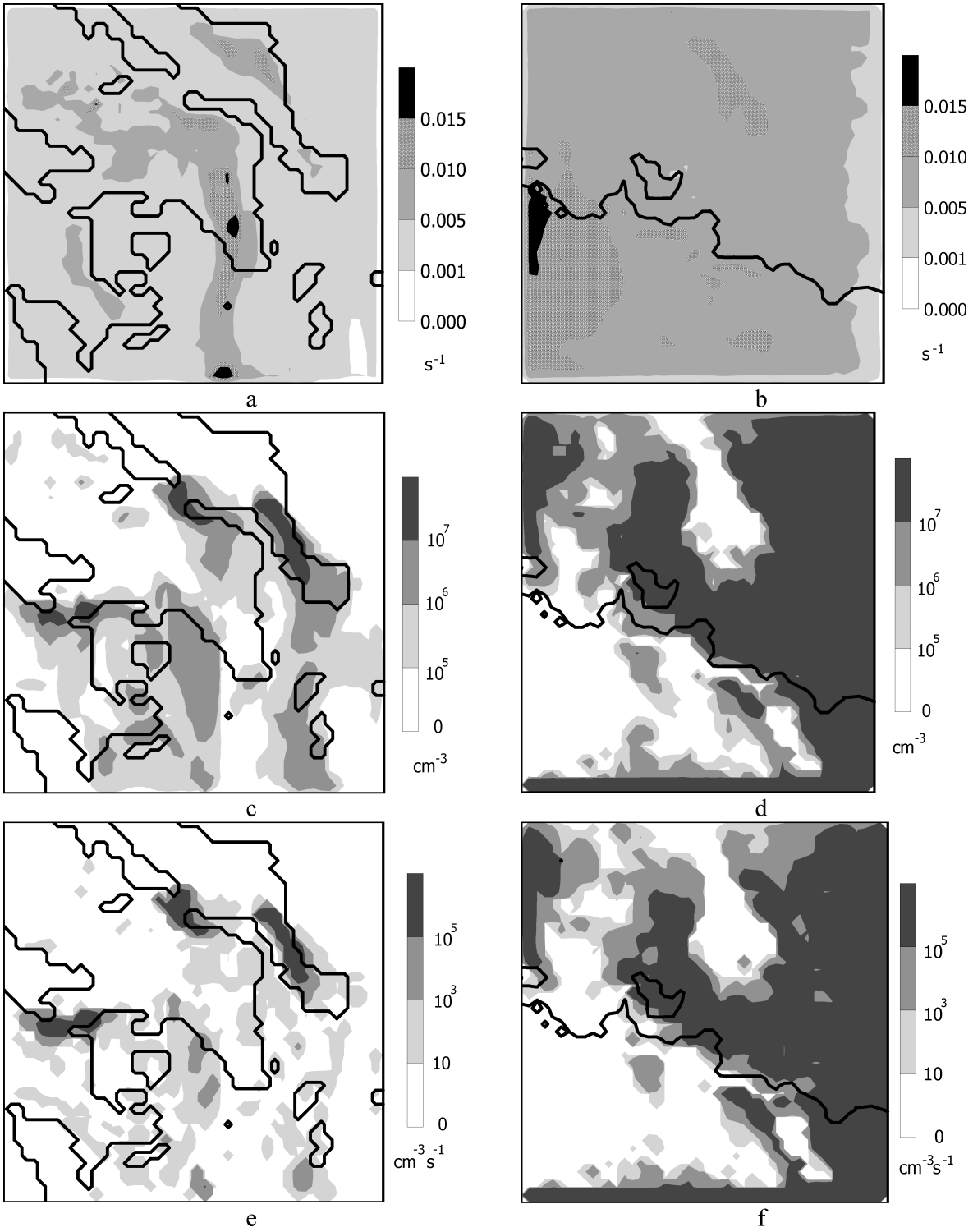

FIG. 1. Spatial distributions of: sulfuric acid condensational sink, sulfuric acid available for new particle formation and the nucleation rate: (a), (c), and (e) at 15:00(LST) on 24 June 2003 for the GAA, and, (b), (d), and (f) at 15:00 (LST) on 8 July 2002 for the GMA, respectively.

areas that are characterized by enhanced flux of gases onto pre-existing particles ("condensational sink"), nuclei growth rates should exceed 10 nm hr^{-1} to avoid coagulation losses onto pre-existing particles (Kulmala et al. 2005). In contrast, a growth rate of 1 nm hr^{-1} is sufficient to avoid losses in very clean environments (Kerminen et al. 2001; Kulmala et al. 2004b).

The nuclei growth parameterization is applied until the new particles are large enough to be introduced into the smallest size

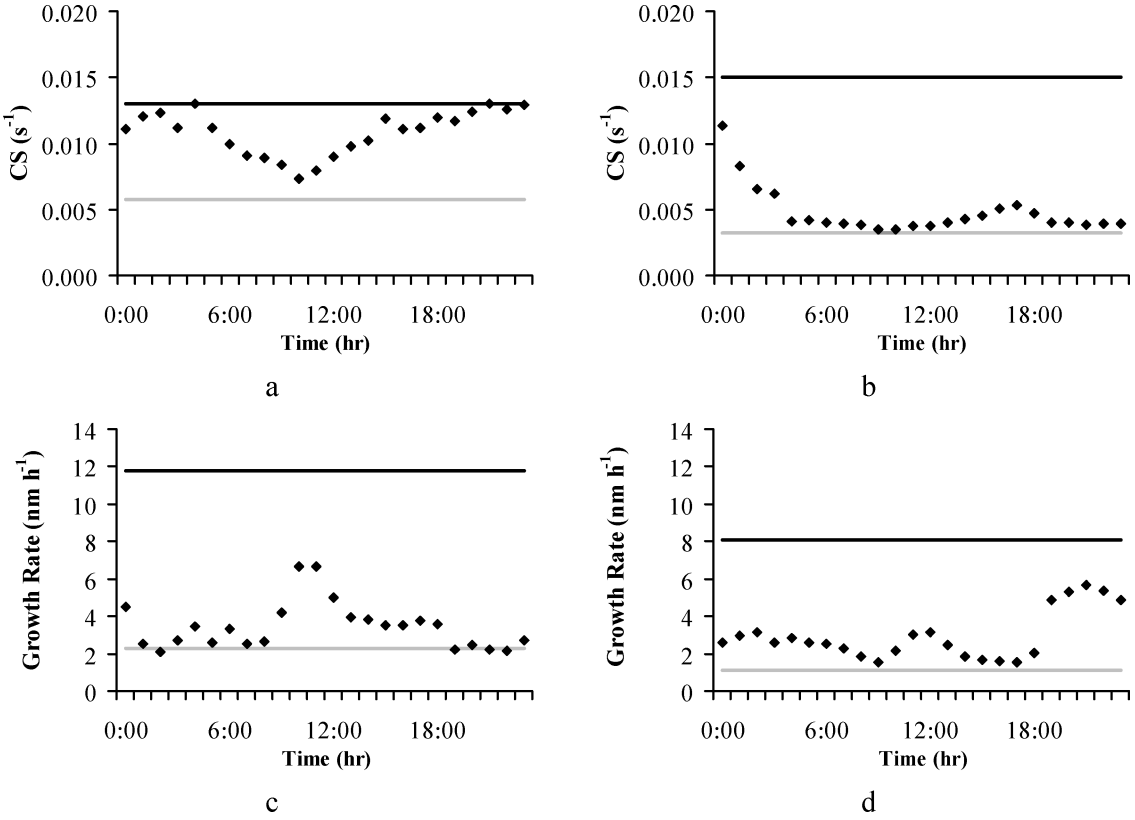

FIG. 2. Comparison of the calculated condensational sink (dots) and growth rate (dots) against observations: (a) and (c) for "Thrakomakedones" monitoring station on 24 June 2003; (b) and (d) for "Plan d' Aups" monitoring station on 8 July 2002, respectively. The black line corresponds to the upper limit of the observations while the grey line corresponds to the lower one.

section of UAM-AERO. This is estimated to happen several times during a day and for several cells of the grid. Figure 3 presents the total organic mass that is introduced into the UAM-AERO aerosol grid over a 24-hour period for the GAA (Figure 3a) and the GMA (Figure 3b), respectively. Comparing the two areas of interest, one observes that more mass crosses the lower diameter in the GAA despite the higher nucleation rate in the GMA. This is due to the limited amount of organic vapors

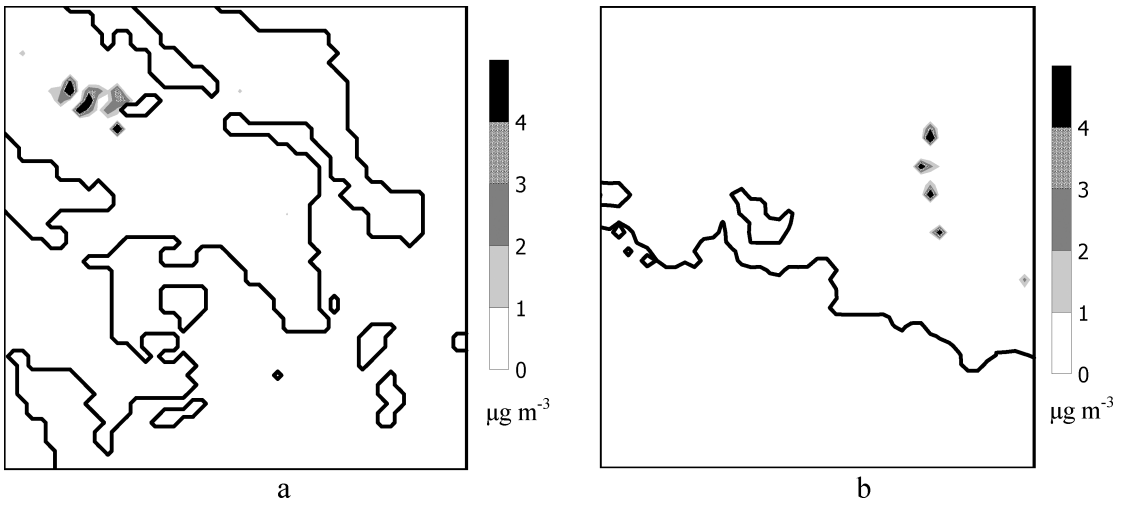

FIG. 3. Total organic mass that is calculated by the model to cross the lower diameter used by UAM-AERO (40 nm) in a 24-hour period, (a) for the GAA episode of 24 June 2003, and, (b) for the GMA episode of 8 July 2002.

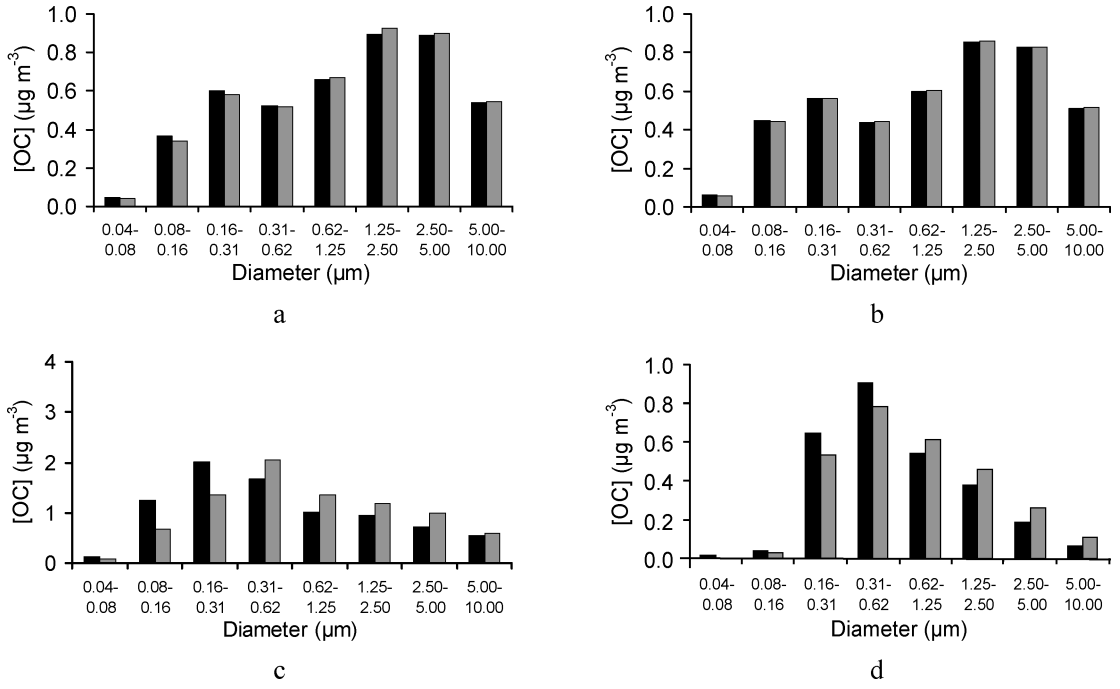

FIG. 4. Spatial average concentrations of secondary organic carbon in each size bin and aerosol size distributions in a cell where nucleation is noted are presented with (black) and without (grey) nucleation: (a) and (c) at 15:00 (LST) on 24 June 2003 for the GAA; (b) and (d) at 15:00 (LST) on 8 July 2002 for the GMA, respectively.

in the GMA that constrains the growth rate; hence nuclei are lost from coagulation onto pre-existing particles. This is consistent with the very low terpene emissions (primary SOA precursors) observed in the GMA.

It should be noted that the SOA mass is not affected by the presence of nucleation; however, the size distribution of the SOA does. More specifically, the new particle formation, as a result of the nucleation and growth processes, leads to increases in the mass concentrations in the smaller size bins, hence decreasing the SOA in the larger size bins. The spatial average concentrations of SOA in each size bin at 15:00 (LST) on June 24, 2003, for the GAA and 15:00 (LST) on July 8, 2002, are presented in Figures 4a and 4b, respectively. Results are shown with and without nucleation present. As expected, the presence of nucleation causes an increase in the fine fraction of SOA. Although this increase is not prevalent everywhere, there are cells in the domain where the size distribution is significantly modified. The results for a cell where nucleation events are noted for GAA and GMA are presented in Figures 4c and 4d, respectively.

Effects of Nucleation on CCN Concentrations

Figure 5 presents the domain-wide CCN spectra (i.e., concentration as a function of supersaturation) for the base case scenario without nucleation (black lines), and the perturbation from nucleation (black bars) for the GAA (Figure 5a) and the GMA (Figure 5b). Results are shown for the whole domain, and for a cell with intense nucleation. We focus our analysis in the 0.1 to 1.2% supersaturation range, as higher or lower values would activate particles outside of the resolved aerosol size range.

The domain-wide change in CCN concentrations at 0.1% supersaturation is 5.5% (from 52 to 55 cm^{-3}) for GAA and 1% (from 455 to 460 cm^{-3}) for GMA, at 0.5% supersaturation is 8% (from 196 to 212 cm^{-3}) for GAA and 2.3% (from 2755 to 2818 cm^{-3}) for GMA, and at 1% supersaturation is 3% (from 1490 to 1536 cm^{-3}) for GAA and 10% (from 4306 to 4722 cm^{-3}) for GMA (Figures 5a and 5b, black bars). Enhancement in areas close and downwind the nucleation events can be as much as 100% for GAA (Figure 5c, black bars) and 40% for GMA (Figure 5d, black bars). This enhancement in our simulations covers approximately 10% of the domains. As it is expected, maximum difference is observed in cells where nucleation takes place while it gradually diminishes downwind of nucleation bursts which in our simulations occur over land.

Comparing the two domains for the scenario with nucleation, higher CCN concentrations are predicted in the GMA; whether this is because of the differences in chemical composition (soluble fraction is 0.26–0.42 in the GMA vs. 0.15–0.25 in the GAA) or aerosol concentration [for the specific episode the 24-hour average for PM10 concentrations is 20 $\mu g\ m^{-3}$ (15–90 $\mu g\ m^{-3}$) for the GAA vs. 38 $\mu g\ m^{-3}$(20–140 $\mu g\ m^{-3}$) for the GMA] can be investigated using the normalized sensitivity of CCN to

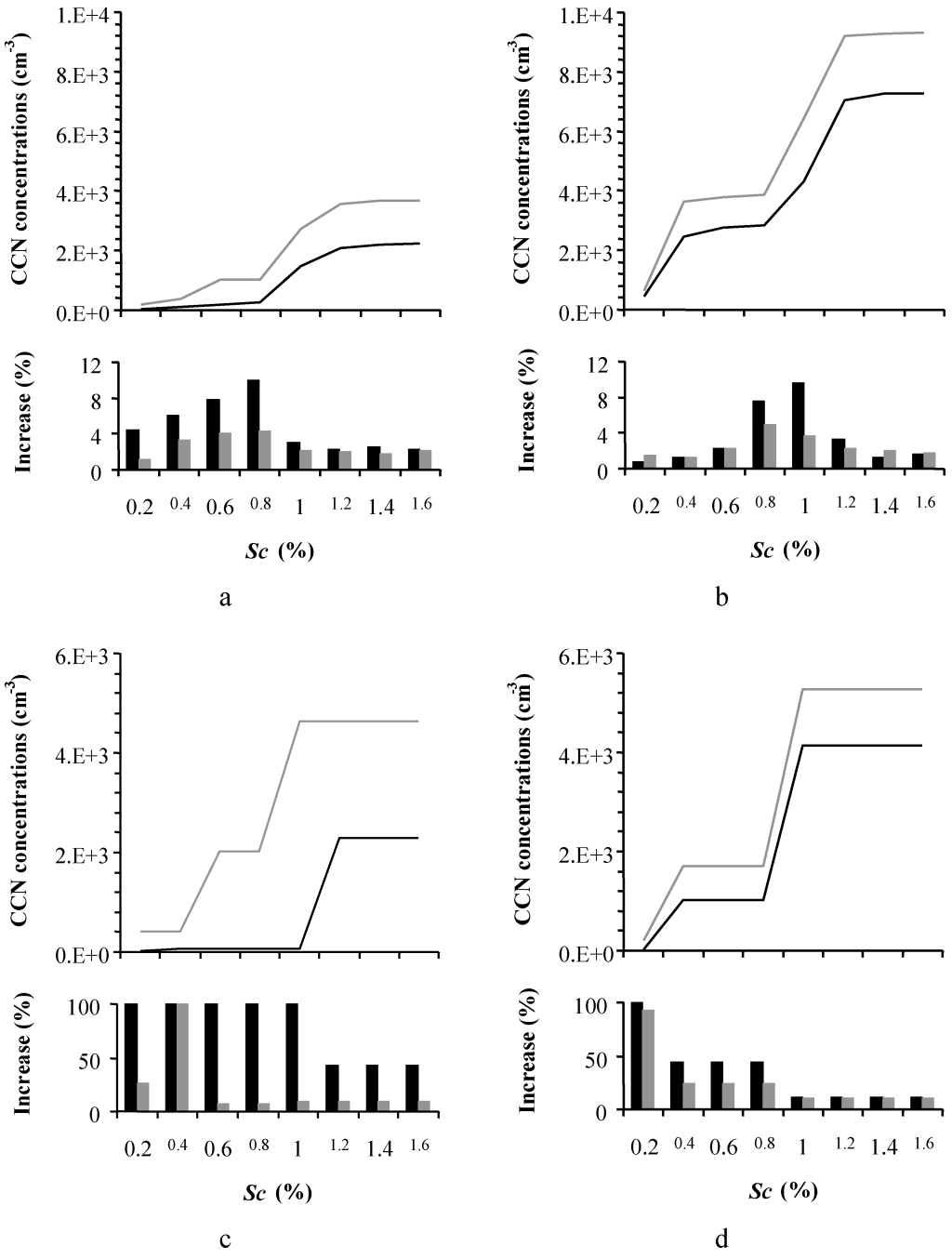

FIG. 5. CCN concentrations as a function of supersaturation (Sc) from simulations neglecting nucleation for two different aerosol chemical compositions: (1) purely inorganic aerosol composition with surface tension equal to that of pure water (black line); (2) a mixture of inorganics and organics (60% of the OC is considered as water soluble) with variable surface tension (grey line). The bar plots represent the net increase due to nucleation for the two different chemical compositions (black and grey bars, respectively) (a) Domain average for the GAA; (b) Domain average for the GMA; (c) Local change for the GAA; (d) Local change for the GMA.

changes in solute fraction. Our analysis (not shown) suggests that 87% of the increase in CCN concentrations is from shifts in the aerosol size distribution and to a lesser extent from changes in the soluble fraction. The implication is that nucleation will most likely always be an important contributor to CCN concentrations for GAA and GMA.

Analysis of satellite images reveals the high frequency of occurrence of stratocumulus and cumulus clouds in these two

areas[1,2] (Stubenrauch et al. 1999; Cartalis et al. 2004); CCN perturbations could affect their radiative properties and precipitation efficiency and have an important impact on the local energy balance, hydrology and climate. Given that the maximum supersaturations in such clouds typically range between 0.1 and 0.8% (Hudson and Svensson 1995; Hoppel et al. 1996; Seinfeld and Pandis 1998), our simulations suggest that nucleation could increase cloud droplet concentrations by 50–100% (Sotiropoulou et al. 2006) in regions close to nucleation events which cover approximately 10% of the domain. In addition to changes in radiative fluxes and precipitation efficiency the perturbed clouds would exhibit higher actinic fluxes above cloud top, and potentially enhance nucleation (Russell et al. 1994); whether or not this feedback is important cannot be addressed with our current modeling framework and is left for future studies.

SENSITIVITY ANALYSIS

Sensitivity of the Size Distribution to Important Thermokinetic Parameters

It is important to examine the sensitivity of our simulations to poorly constrained parameters affecting nucleation and SOA production. These are (i) the value of vaporization enthalpy, H, since it strongly impacts partitioning of COC, and (ii) the condensable species accommodation coefficient, α which determines the flux of sulfuric acid and organic vapors onto pre-existing particles. H was varied between 10 and 25 kcal mol^{-1}, based on the results of Sheehan and Bowman (2001). Moreover, we performed an additional simulation, keeping the aerosol yield constant, independently of the temperature and the pre-existing mass, as in the original version of UAM-AERO. The accommodation coefficient was varied between 0.01 and 1.

Figure 6 presents the sensitivity of the condensational sink and the growth rate to H and α for the GAA (Figures 6a and 6c) and GMA (Figures 6b and 6d), respectively. The results show that although changes in vaporization enthalpy affect the mass of SOA formed, they do not have a significant impact on the condensational sink and the growth rate, that is, on the size distribution. More specifically, an increase in the value of vaporization enthalpy causes a subsequent increase in the quantity of COC produced and vice-versa. On the contrary, changes in the accommodation coefficient do not impact SOA mass but substantially modify the size distribution. This insensitivity allows for changes in the chemistry for SOA formation without affecting the results of the nucleation and growth modules. On the other hand, *CS* and *GR* are very sensitive to changes in α (Equations [10, 11, 12]). When values of α lower than unity are used, the simulated *CS* (Figure 6a and 6b) and *GR* (Figure 6c and 6d) strongly disagree with observations for both GAA and GMA; this suggests that the appropriate value of α in the growth parameterization is unity.

Sensitivity of CCN to Organic Solubility

A basic assumption made in the calculation of CCN concentrations is that organics are insoluble. However, numerous studies suggest that a fraction of OC is water-soluble (e.g., Cruz and Pandis 1997; Zappoli et al. 1999; Decesari et al. 2001; Sullivan et al. 2004) and could impact the CCN activity of aerosol (e.g., Rivera-Carpio et al. 1996; Corrigan and Novakov 1999). Introducing the interaction of organics with water into Köhler theory is far from trivial; organics can affect CCN characteristics by reducing droplet surface tension and contributing soluble material (Shulman et al. 1996; Li et al. 1998; Facchini et al. 1999; Facchini et al. 2000; Nenes et al. 2002; Lance et al. 2004). Mircea et al. (2002) estimated that under typical atmospheric supersaturations, including the surface tension effects of water soluble organic compounds may increase the CCN number concentration by up to 13% for a marine aerosol, by up to 97% for a rural aerosol and by up to 110% for an urban aerosol. We examine the sensitivity of our simulations to the organic solubility and its effect on surface tension. For this, we consider that 60% of OC is water-soluble; this is consistent with measurements of Sullivan et al. (2004) for the Eastern United States and Zappoli et al. (1999) for polluted European polluted sites. In addition, we assume the water-soluble organic to depress surface tension, using the empirical correlation of Facchini et al. (1999):

$$\sigma_s = 72.8 - 0.0187T \ln(1 + 628.14C) \qquad [20]$$

where σ_s is the surface tension of the CCN, and C is the concentration of dissolved carbon (in mol l^{-1}).

Figure 5 presents the domain-wide CCN spectra for the scenario that 60% of OC is water-soluble without nucleation (grey lines), and the perturbation from nucleation (grey bars) for the GAA (Figure 5a) and the GMA (Figure 5b). The presence of soluble organics and reduction in the surface tension decreases the critical supersaturation (3–40% for the GAA and 1–9% for the GMA depending on the size section), resulting in a CCN increase of approximately 130% for the GAA (Figure 5a) and of 40% for the GMA (Figure 5b) (at 0.8% supersaturation). Comparing the two scenarios (pure inorganic and organic +

[1]Analysis of infrared (IR) sounders (TIROS-N Operational Vertical Sounder observations from the National Oceanic and Atmospheric Administration (NOAA) polar-orbiting environmental satellites) and detailed comparisons between cloud parameters obtained from this global dataset, (NOAA–National Aeronautics and Space Administration Pathfinder Program) with time–space-collocated observations of clouds from the reprocessed International Satellite Cloud Climatology Project (ISCCP) dataset, classifies stratocumulus and cumulus clouds as frequent cloud types for South France (Stubenrauch et al. 1999).

[2]Data from the Advanced Very High Resolution Radiometer (AVHRR) on board the National Oceanic and Atmospheric Administration (NOAA) satellites coupled with synoptic maps (12:00 UTC) from the European Centre for Medium-Range Weather Forecasts (ECMWF) where used for the categorizations of cloud feature formed by each of the four prevailing weather types in the area of Greece and demonstrated stratocumulus and cumulus clouds as frequent cloud types (Cartalis et al. 2004).

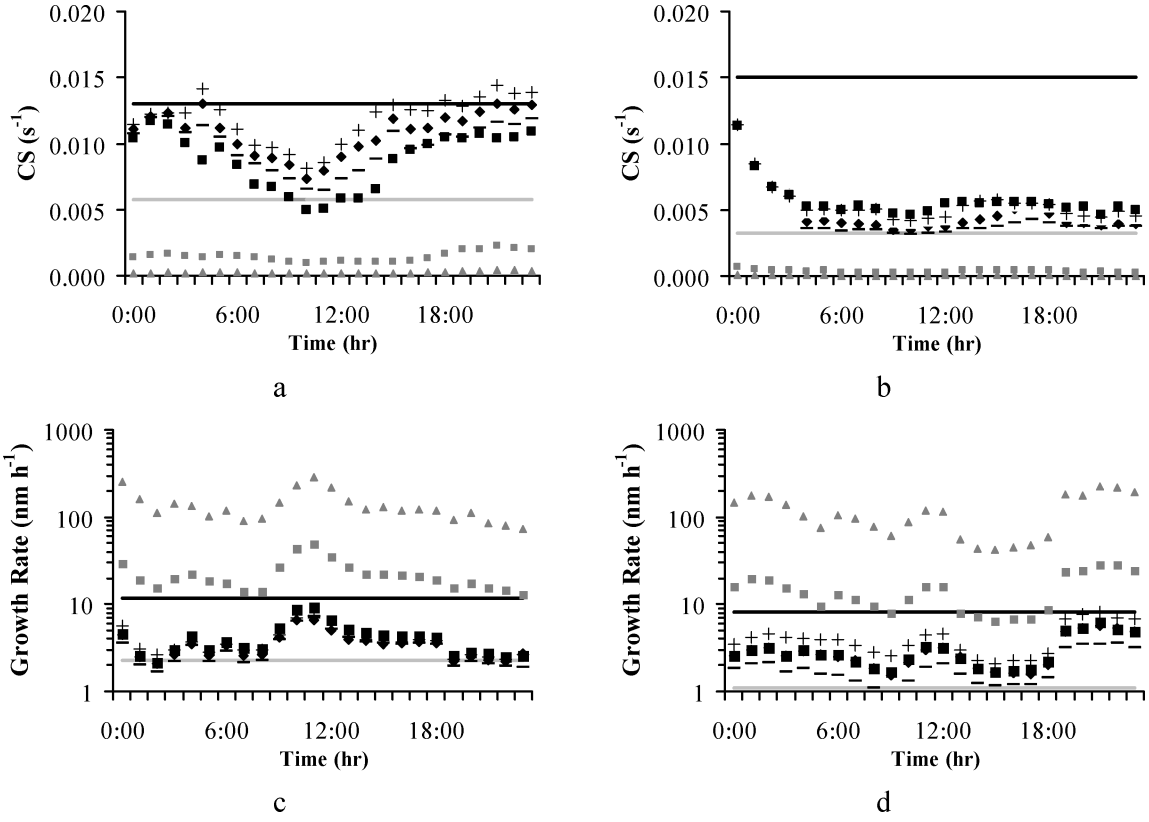

FIG. 6. Results of the sensitivity analysis for the condensational sink and growth rate (a) and (c) for "Thrakomakedones" monitoring station on 24 June 2003; (b) and (d) for "Plan d' Aups" monitoring station on 8 July 2002, respectively. The black line corresponds to the upper limit of the observations while the grey line corresponds to the lower one; also shown the results of: the base case (♦), considering a constant OC yield (■), H equal to 10 (−) and to 25 (+), accommodation coefficients equal to 0.01 (▲) and 0.1 (■).

inorganic), we found an average increase in the soluble fraction of around 110% for the GAA and 75% for the GMA. The higher increase in GAA is consistent with the presence of higher amounts of organics in the GAA compared to the GMA, as described above. In areas where nucleation takes place, the effect of water-soluble OC on the CCN spectra is also very important for both the GAA (Figure 5c) and the GMA (Figure 5d).

The net average spatial impact of nucleation for both scenarios [pure inorganics (black bars) and inorganics + organics (grey bars)] is illustrated in the bar plots for each supersaturation for the GAA (Figure 5a) and the GMA (Figure 5b). The domain-wide change in CCN concentrations at 0.1% supersaturation is 2% (from 202 to 206 cm^{-3}) for GAA and 1.5% (from 640 to 650 cm^{-3}) for GMA, at 0.5% supersaturation is 4% (from 1022 to 1065 cm^{-3}) for GAA and 2% (from 3770 to 3860 cm^{-3}) for GMA, and at 1% supersaturation is 2% (from 2737 to 2798 cm^{-3}) for GAA and 4% (from 6443 to 6680 cm^{-3}) for GMA (Figures 5a and 5b, grey bars). Although the spatial average increase is not very high, there are cells in the domain where the CCN concentrations are significantly modified. The net increase (%) for a cell where nucleation events are noted for GAA and GMA are presented in the bar plots of Figures 5c and 5d, respectively. In these areas the enhancement in CCN concentrations can be up to 100% for GAA and 30% for GMA at 0.5% supersaturation. The increase (%) in CCN concentrations due to nucleation seems to be more important for the scenario with pure inorganics; this is the result of the lower number concentrations compared to the scenario with organics and inorganics. In absolute values, the increase is more important for the scenario with organics and inorganics which is consistent with theory (e.g., Mircea et al. 2002).

In order to investigate whether the increase in the CCN concentrations is caused by the increase of the soluble fraction or by changes in the aerosol number concentrations, we used the normalized sensitivity of the CCN concentrations to the increase in solute fraction (not shown). As in the base case scenario, we found that the increase in CCN concentrations when nucleation is considered is mainly (85%) caused by shifts in the aerosol size distribution and in a lesser extend by changes in the soluble fraction, confirming the fact that nucleation will most likely have an impact on CCN concentrations.

SUMMARY AND CONCLUSIONS

The air quality model UAM-AERO has been extended to include the process of new particle formation. New clusters are

assumed to be formed by ternary nucleation of sulfuric acid, ammonia, and water, while the subsequent growth of clusters to large sizes is driven by condensation of sulfuric acid and organic vapors onto the clusters, based on nano–Köhler theory (Kerminen et al. 2004). Both of these processes have been parameterized, allowing a computationally efficient calculation of the flux of new particles to the smallest size bin used for particles by the UAM-AERO model. However, due to coagulational losses of the growing clusters onto pre-existing particles, only a limited number of them manage to grow beyond the minimum diameter used for aerosol treatment by UAM-AERO. Lack of sulfuric acid or organic vapors in the gas phase inhibit the formation of new particles. When the particles cross the lower diameter used by UAM-AERO, their mass is added to the appropriate size bin of each cell. The modifications were shown to have a minimal impact (5–10% increase) on memory usage and computational cost.

The model was used to study the effects of new particle formation on the air quality in the Athens, Greece (GAA) and the Marseilles, France (GMA) greater areas under episodic conditions. Simulations suggest higher sulfuric acid condensational sink and higher remaining quantity of sulfuric acid, available for the nucleation, in the GMA. This is due to the substantially higher SO_2 emissions in the GMA. As a result, the nucleation rate is greater therein compared to the corresponding value for the GAA. The calculated condensational sinks and growth rates of nuclei agree well with observations in the two areas of interest (Kulmala et al. 2004a). Due to the limited quantities of organic vapors, as a result of lower emissions of organic precursors in the GMA, more mass crosses the lower diameter used by UAM-AERO in the GAA, (even though the nucleation rate is higher for the GMA). The inclusion of the new module did not change the total mass of particulate matter in the domain, but did change its distribution in the different size bins; the average mass of the smaller particles in the domain is increased, while the mass of the larger ones is decreased.

Calculations were performed for three values of vaporization enthalpy, three values of accommodation coefficient, and for SOA constant formation yield equal to 762 $\mu g\,m^{-3}$. It was shown that decreasing the accommodation coefficient by a factor of 10 leads to changes in the *CS* and *GR* by an order of magnitude. Values of α other than unity, lead to unrealistic results. Changes in H, although affecting SOA formation, do not have a significant impact on *CS* and *GR* and thus do not affect the quantity of organic carbon formed by nucleation.

Nucleation impacts the aerosol size distribution and CCN concentrations. The results of our simulations indicate that CCN at 1% supersaturation can increase by more than 100% in the GAA, and more than 40% in the GMA. CCN concentrations are also affected by organic solubility. However, the relative importance of nucleation on the CCN concentrations is not influenced by organic solubility. This suggests that clouds downwind of nucleation bursts are likely to be considerably affected regardless of the oxidation state of OC condensing onto the particles. Moreover, the effects of nucleation are locally more important than changes of hygroscopicity from ageing of the particles. In addition to changes in the local energy balance and precipitation efficiency, the regions above perturbed clouds can increase actinic fluxes and potentially enhance nucleation; the importance of these perturbations requires a simulation with a coupled regional climate model and will be the focus of a future study.

REFERENCES

Adams, P. J., and Seinfeld, J. H. (2002). Predicting Global Aerosol Size Distributions in General Circulation Models, *J. Geophys. Res.* 107 (D19), DOI: 10.1029/2001JD001010.

Bartzis, J. G., Venetsanos, A., Varvayanni, M., Catsaros, N., and Megaritou, A. (1991). ADREA-I. A Transient Three-Dimensional Transport Code for Complex Terrain and Other Applications, *Nucl. Technol*., 94:135–148.

Bartzis, J. G., Andronopoulos, S., Kulmala, M., Larsen, B., Lazaridis, M., Lohse, C., Mirabel, P., and Pilinis, C. (2004). The Bond Project: The Marseille and Athens Experimental Campaign. An Overview. European Aerosol Conference (EAC'2004), Budapest, Hungary, September 2004.

Breinbjer, B., Astorga-Llorens, C., Van Dingenen, R., Wintherhalter, R., and Larsen, B. (2003). Secondary Organic Aerosols Formation from Ozonolysis of α-Pinene: Temperature Dependence of Mass and Product Yields from 281 K to 307 K, European Aerosol Conference, Madrid, September 2003.

Cartalis, C., Chrysoulakis, N., Feidas, H., and Pitsitakis, N. (2004). Categorization of Cold Period Weather Types in Greece on the Basis of the Photointerpretation of NOAA/AVHRR Imagery, *Int. J. Remote Sensing*, 25:2951–2977, DOI: 10.1080/ 01431160310001632684.

Carter, W. P. L. (1990). A Detailed Mechanism for the Gas-Phase Atmospheric Reactions of Organic Compounds, *Atmos. Environ.* 3:481–518.

Charlson, R. J., Lovelock, J. E., Andreae, M. O., and Warren, S. G. (1987). Ocean Phytoplankton, Atmospheric Sulfur, Cloud Albedo and Climate, *Nature* 326:655–661.

Corrigan, C. E., and Novakov, T. (1999). Cloud Condensation Nucleus Activity of Organic Compounds: A Laboratory Study, *Atmos. Environ.* 33:2661–2668.

Cruz, C. N., and Pandis, S. N. (1997). A Study of the Ability of Pure Secondary Organic Aerosol to Act as Cloud Condensation Nuclei, *Atmos. Environ.* 31:2201–2214.

Decesari, S., Facchini, M. C., Matta, E., Lettini, F., Mircea, M., Fuzzi, S., Tagliavini, E., and Putaud, J.-P. (2001). Chemical Features and Seasonal Variation of Fine Aerosol Water-Soluble Organic Compounds in the Po Valley, Italy, *Atmos. Environ.* 35, 3691– 3699.

ENVIRON. (2004). User's Guide to the Comprehensive Air Quality Model with Extensions (CAMx), version 4.10s, ENVIRON International Corporation, California.

EPA. (1999). Science Algorithms of the EPA Models-3 Community Multiscale Air Quality (CMAQ) Modeling System. EPA/600/R-99/030, March 1999.

Facchini, M. C., Decesari, S., Mircea, M., Fuzzi, S., and Loglio, G. (2000). Surface Tension of Atmospheric Wet Aerosol and Cloud/For Droplets in Relation to their Organic Carbon Content and Chemical Composition, *Atmos. Environ.* 34:4853–4857.

Facchini, M. C., Mircea, M., Fuzzi, S., and Charlson, R. J. (1999). Cloud Albedo Enhancement by Surface-Active Organic Solutes in Growing Droplets, *Nature* 401:257–259.

Griffin, R. J., Dabdud, D., Kleeman, M. J., Fraser, M. P., Cass, G. R., and Seinfeld, J. H. (2002). Secondary Organic Aerosol 3. Urban/regional Scale Model of Size- and Composition Resolved Aerosols, *J. Geophys. Res.* 107(D17), DOI:10.1029/2001JD000544.

Hegg, D. A. (1990). Heterogeneous Production of Cloud Condensation Nuclei in the Marine Atmosphere, *Geophys. Res. Lett.* 17:2165–2168.

Henning, S., Weingartner, E., Nyeki, S., Schwikowski, M., Baltensperger, U., and Gäggeler, H. W. (1999). Size Dependent Activation of Aerosol Particles

to Cloud Droplets at the High Alpine Site Jungfraujoch (3580 m asl), High-Alpine Ecology Conference 1999.

Hoppel, W. A., Frick, G. M., and Fitzgerald, J. W. (1996). Deducing Droplet Concentration and Supersaturation in Marine Boundary Layer Clouds from Surface Aerosol Measurements, *J. Geophys. Res.* 101(D21):26553–26566, 10.1029/96JD02243.

Hudson, J. G., and Svensson, G. (1995). Cloud Microphysical Relationships in California Marine Stratus, *J. Appl. Meteor.* 34:2655–2666.

Hudson, J. G., and Da, X. Y. (1996). Volatility and Size of Cloud Condensation Nuclei, *J. Geophys. Res.* 101:4435–4442.

Jang, M., Czoschke, N. M., Lee, S., and Kamens R. M. (2003). Heterogeneous Atmospheric Aerosol Production by Acid-Catalyzed Particle-Phase Reactions, *Science* 298:814–817.

Kerminen, V.-M., and Kulmala, M. (2002). Analytical Formulae Connecting the "Real" and the "Apparent" Nucleation Rate and the Nuclei Number Concentration for Atmospheric Nucleation Events. *J. Aerosol Sci.* 33:609–622.

Kerminen, V.-M., Pirjola, L., and Kulmala, M. (2001). How Significantly does Coagulational Scavenging Limit Atmospheric Particle Production? *J. Geophys. Res.* 106:24,119–24,126.

Kerminen, V.-M., Antilla, T., Lehtinen, K. E. J., and Kulmala, M. (2004). Parameterization for Atmospheric New-Particle Formation: Application to a System Involving Sulfuric Acid and Condensable Water-Soluble Organic Vapors, *Aerosol Sci. Technol.* 38:1001–1008.

Kim, C. S., Adachi, M., Okuyama, K., and Seinfeld, J. H. (2002). Effect of NO2 on Particle Formation in SO2/H2O/air Mixtures by Ion-Induced and Homogenous Nucleation, *Aerosol Sci. Technol.* 36:941–952.

Kirkevåk, A., and Iversen, T. (2002). Global Direct Radiative Forcing by Process-Parameterized Aerosol Optical Properties, *J. Geophys. Res.* 107 (D20), DOI: 10.1029/2001JD000886.

Köhler, H. (1936). The Nucleus in the Growth of Hygroscopic Droplets, *Trans. Far.* Soc. 32:1152–1161.

Kulmala, M., and Laaksonen, A. (1990). Binary Nucleation of Water-Sulfuric Acid System: Comparison of Classical Theories with Different H_2SO_4 Saturation Vapor Pressure, *J. Phys. Chem.* 93:696–701.

Kulmala, M., Petäjä, T., Mönkkönen, P., Koponen, I. K., Dal Maso, M., Alto, P. P., Lehtinen K. E. J., and Kerminen, V. M. (2005). On the Growth of Nucleation Mode Particles: Source Rates of Condensable Vapor in Polluted and Clean Environments, *Atmos. Chem. Phys.* 5:409–416.

Kulmala, M., Pirjola, L., and Mäkelä, J. M. (2000). Stable Sulfate Clusters as a Source of New Atmospheric Particles, *Nature* 404:66–69.

Kulmala, M., Vehkamäki, H., Petäjä, T., Dal Maso, M., Lauri, A., Kerminen, V.-M., Birmili, W., and McMurry, P. H. (2004a) Formation and Growth Rates of Ultrafine Atmospheric Particles: A Review of Observations, *J. Aerosol Sci.* 35:143–176.

Laakso, L., Kulmala, M., and Lehtinen, K. E. J. (2003). The Effect of Condensation Rate Enhancement Factor on 3-nm Particle Formation in Binary ion-induced and homogeneous nucleation, *J. Geophys. Res.* 108 (D18), DOI: 10.1029/2003JD003432.

Laaksonen, A., Hamed, A., Joutsensaari, J., Hiltunen, L., Cavalli, F., Junkermann, W., Asmi, A., Fuzzi, S., Facchini, M. C. (2005). Cloud Condensation Nucleus Production from Nucleation Events at a Highly Polluted Region, *Geoph. Res. Lett.* 32, L06812, DOI: 10.1029/2004GL022092.

Lance, S., Nenes, A., and Rissman, T. (2004). Chemical and Dynamical Effects on Cloud Droplet Number: Implications for Estimates of the Aerosol Indirect Effect., *J. Geoph. Res.*, 109, D22208, DOI:10.1029/2004JD004596.

Larsen, B. R. Breinbjerg, B., Astorga, C., Duane, M., Hjorth, J., Van Dingenen, R., Svendby, T., and Lazaridis, M. (2003). "Sources for Ambient Particulate Matter. I. Gas-to-Particle Conversion of Biogenic Compounds." Report EUR 20743 EN.

Li, Z., Williams, A. L., and Rood, M. J. (1998). Influence of Soluble Surfactant Properties on the Activation of Aerosol Particles Containing Inorganic Solute, *J. Atmos. Sci.* 55:1859–1866.

Lin, X., and Chameides, W. L. (1993). CCN Formation from DMS Oxidation without SO_2 Acting as an Intermediate, *Geophys. Res. Lett.* 20:579–582.

Lowenthal, D. H., Borys, R. D., and Wetzel, M. A., (2002). Aerosol Distributions and Cloud Interactions at a Mountaintop Laboratory, *J. Geophys. Res.*, 107(D18), 4345, DOI:10.1029/2001JD002046.

Medina, J., Cottrell, L., Griffin, R., Beckman, P. J., Ziemba, L. D., and Nenes, A., Cloud Condensation Nuclei (CCN) Closure on New England Ambient Aerosol During the ICARTT 2004 Field Campaign: a) Effects of Size-Dependent Composition, *J. Geophys. Res.*, in review.

Meng, Z., Dabdub, D., and Seinfeld, J. H. (1998). Size-Resolved and Chemically Resolved Model of Atmospheric Aerosol Dynamics, *J. Geophys. Res.* 103:3419–3435.

Meskhidze, N., A. Nenes, Conant, W. C., and Seinfeld, J. H. (2005). Evaluation of a new Cloud Droplet Activation Parameterization with In Situ Data from CRYSTAL-FACE and CSTRIPE, *J. Geoph. Res.* 110, D16202, DOI:10.1029/2004JD005703.

Mircea, M., Facchini, M. C., Decesari, S., Fuzzi, S., and Charlson, R. J. (2002). The Influence of the Organic Aerosol Component on CCN Supersaturation Spectra for Different Aerosol Types, *Tellus, Series B*, 54:74–81.

Napari, I., Noppel, M., Vehkamäki, H., and Kulmala, M. (2002a). An Improved Model for Ternary Nucleation of Sulfuric Acid-Ammonia-Water, *J. Chem. Phys.* 116:4221–4227.

Napari, I., Noppel, M., Vehkamäki, H., and Kulmala, M. (2002b). Parameterization of Ternary Nucleation Rates for H2SO4–NH3–H2O Vapors, *J. Geophys. Res.* 107:4381–4386, DOI: 10.1029/2002JD002132.

Nenes, A. Charlson, R. J., Facchini, M. C., Kulmala, M., Laaksonen, A., Seinfeld, J.H. (2002) Can Chemical Effects on Cloud Droplet Number Rival the First Indirect Effect? *Geoph. Res. Lett.* 29 (17), 1848, DOI: 10.1029/2002GL015295

Nenes, A., Pandis, S. N., and Pilinis, C. (1999). Continued Development and Testing of a New Thermodynamic Aerosol Module for Urban and Regional Air Quality Models, *Atmos. Environ.* 33:1553–1560.

Nenes, A., Pilinis, C., and Pandis, S. N. (1998). ISORROPIA: A New Thermodynamic Model for Inorganic Multicomponent Atmospheric Aerosols, *Aquat. Geochem.* 4:123–152.

O'Dowd, C. D., Hämeri, K., Mäkelä, J. M., Pirjola, L., Kulmala, M., Jennings, S. G., Berresheim, H., Hansson, H.-C., De Leeuw, G., Kunz, G. J., Allen, A. G., Hewitt, C. N., Jackson, A., Viisanen, Y., and Hoffmann, T. (2002). A Dedicated Study of New Particle Formation and Fate in the Coastal Environment (PARFORCE): Overview of Objectives and Achievements, *J. Geophys. Res.* 107(D19), 8108, DOI:10.1029/2001JD000555.

O'Dowd, C. D., Lowe, J. A., and Smith, M. H. (1999). Coupling Sea-Salt and Sulphate Interactions and its Impact on Cloud Droplet Concentration Predictions, *Geophys. Res. Lett.* 26:1311–1314.

Odum, J. R., Hoffmann, T., Bowman, F., Collins, D., Flagan, R. C., and Seinfeld, J. H. (1996). Gas/Particle Partitioning and Secondary Organic Aerosol Yields, *Environ. Sci. Technol.* 30:2580–2585.

Peters, A., Wichmann, E., Tuch, T., Heinrich, J., and Heyder, J. (1997). Respiratory Effects are Associated with the Number of Ultrafine Particles, *Am. J. Respir. Crit. Care Med.* 155:1276–1383.

Pirjola, L., O'Dowd, C. D., and Kulmala, M. (2002). A Model Prediction of the Yield of Cloud Condensation Nuclei from Coastal Nucleation Events, *J. Geophys. Res.* 107 (D19), DOI:10.1029/2000JD000213.

Rivera-Carpio, C. A., Corrigan, C. E., Novakov, T., Penner, J. E., Rogers, C. F., and Chow, J. C. (1996). Derivation of Contributions of Sulfate and Carbonaceous Aerosols to Cloud Condensation Nuclei from Mass Size Distributions, *J. Geophys. Res.* 101 19483–19493.

Russell, L. M., Pandis, S. N., and Seinfeld, J. H. (1994). Aerosol Production and Growth in the Marine Boundary Layer, *J. Geophys. Res.* 99:20989–21003.

SAI (System Applications International) (1990). User's Guide for the Urban Airshed Model, Volume I. Prepared by Systems Applications International (Report No. SYSAPP-90/018 a, b, c, d, e), San Rafael, CA, a, b, c, d, e.

Schell, B., Ackermann, I. J., Hass, H., Binkowski, F. S., and Ebel A. (2001). Modeling the Formation of Secondary Organic Aerosol within a Comprehensive Air Quality Model System, *J. Geophys. Res.* 106:28275–28293.

Schwartz, J., Dockery, D. W., and Neas, L. M. (1996). Is Daily Mortality Associated Specifically with Fine Particles? *J. Air Waste Manag. Assoc.* 46:927–939.

Shaw, G. E., Benner, R. L., Cantrell, W., and Clarke, A. D. (1998). On the Relation of Climate: A Sulfate Particle Feedback Loop Involving Deep Convection, *Climate Change* 39:23–33.

Shulman, M., Jacobson, M. C., Carlson, R. J., Synovec, R. E., and Young, T. E. (1996). Dissolution Behavior and Surface Tension Effects of Organic Compounds in Nucleating Cloud Droplets, *Geophys. Res. Lett*. 23:277–280.

Sonoma Technology, Inc. (1996). User's Guide to the UAM-AERO Model. STI-93110-1600-UG.

Sotiropoulou, R. E. P., Medina, J., and Nenes, A. (2006). CCN Predictions: Is Theory Sufficient for Assessments of the Indirect Effect? *Geoph. Res. Lett*. 33, L05816, DOI:10.1029/2005GL025148.

Sotiropoulou, R. E. P., Tagaris, E., Pilinis, C., Andronopoulos, S., Sfetsos, A., and Bartzis, J. G. (2004a). The BOND Project: Biogenic Aerosols and Air Quality in Athens and Marseille Greater Area, *J. Geophys. Res*. 109, D05205, DOI:10.1029/2003JD003955.

Sotiropoulou, R. E. P., Tagaris, E., Pilinis, C., Andronopoulos, S., Sfetsos, A., and Bartzis, J. G., (2004b). The BOND Project: Contribution of Biogenic Emission to the Aerosol Budget in the Mediterranean Area, European Aerosol Conference (EAC2004), Budapest, Hungary, September 2004.

Stanier, C. O., Khlystov, A. Y., and Pandis, S. N. (2004). Nucleation Events During the Pittsburg Air Quality Study: Description and Relation to Key Meteorological, Gas Phase, and Aerosol Parameters, *Aerosol Sci. Technol*.38(S1):253–264.

Sullivan, A. P., Weber, R. J., Clements, A. L., Turner, J. R.. Bae, M. S., and Schauer, J. J. (2004). A Method for On-Line Measurement of Water Soluble Organic Carbon in Ambient Aerosol Particles: Results from an Urban Site, *Geophys. Res. Lett*. 31, L13105, DOI:10.1029/2004GL019681.

Twomey, S. (1974). Pollution and the Planetary Albedo, *Atmos. Environ*. 8, 1251–1256.

Weber, R. J., McMurry, P. H., Mauldin, L., Tanner, D., Eisele, F., Clarke, A. D., and Kapustin, V. N. (1999). New Particle Formation in the Remote Troposphere: A Comparison of Observations at Various Sites, *Geophys. Res. Lett*. 26:307–310.

Yu, F., and Turco, R. P. (2001). From Molecular Clusters to Nanoparticles: Role of Ambient Ionization in Tropospheric Aerosol Formation, *J. Geophys. Res*. 106:4797–4814.

Zappoli, S., Andracchio, A., Fuzzi, S., Facchini, M. C., Gelencsér, A., Kiss, G., Krivácsy, Z., Molnár, Á., Mészáros, E., Hansson, H.-C., Rosman, K., and Zebühr, Y. (1999). Inorganic, Organic and Macromolecular Components of Fine Aerosol in Different Areas of Europe in Relation to their Water Solubility, *Atmos. Environ*. 33:2733–2743.

Zhang, K. M., and Wexler, A. S. (2002). A Hypothesis for Growth of Fresh Atmospheric Nuclei, *J. Geophys. Res*. 107 (D21), DOI: 10.1029/2002JD002180.

Zhang, Q., et al. 2004. Insights into Chemistry of Nucleation Bursts and New Particle Growth Events in Pittsburgh Based on Aerosol Mass Spectrometry, *Environ. Sci. Technol*. 38, 4797–4809.

Zhang, Y., Seigneur, C., Seinfeld, J. H., Jacobson, M., Clegg, S. L., and Binkowski, F. S. (2000). A Comparative Review of Inorganic Aerosol Thermodynamic Equilibrium Modules: Similarities, Differences and Their Likely Causes, *Atmos. Environ*. 34:117–137.